PHYSICAL REVIEW B VOLUME 24, NUMBER 10 15 NOVEMBER 1981

# Theoretical study of the electronic structure of GaP(110)

F. Manghi, C. M. Bertoni, C. Calandra, and E. Molinari
*Istituto di Fisica, Università di Modena, 41100 Modena, Italy*
(Received 13 February 1981)

A self-consistent pseudopotential approach has been used to calculate the electronic structure of GaP(110) surface in both ideal and relaxed configurations. Calculations have been performed using the repeated slab method and a local form of the bare ionic pseudopotential. An efficient self-consistent procedure, which allows us to obtain quick convergence and eliminates some difficulties found in previous applications of the method, has been used. Particular care has been devoted to have complete consistency between bulk and slab calculations. Our results for the ideal surface show various surface states, whose distribution and nature are similar to those found in tight-binding calculations. For the geometry of the relaxed surface we assumed a rotation-relaxation model determined by a recent low-energy electron diffraction study. With this geometry our results show that a nonvanishing density of empty surface states, to a large extent due to backbonds, remains in the gap. The orbital composition of these states, as well as of all the other surface features, is detailed, together with the mirror-plane symmetries relevant in the interpretation of angle-resolved photoemission data. Our results are in agreement with the experimental data provided by various different measurements.

## I. INTRODUCTION

This paper will report on a theoretical investigation of the electronic structure of the (110) surface of GaP. This surface appears to be somewhat different from the (110) surface of other III-V compounds, in that it shows a nonvanishing density of empty surface states in the band gap, even in absence of cleavage defects. Contact potential difference and photon-threshold measurements[1] indicate that the Fermi level is pinned on $n$-type GaP(110). Such a situation does not occur for the other semiconducting compounds, unless cleavage defects or chemisorbed impurities give rise to extrinsic states in the gap. This conclusion is supported by photoemission yield spectroscopy data,[2] by which the existence of a low-density tail of an intrinsic surface-state band near the conduction-band minimum has been proved. Photoemission partial-yield data[3] and energy-loss spectra[4] can be understood assuming that the final state is an empty band in the gap, provided that the exciton binding energy for core-level transition is about 0.5 eV.

It is now well established that the absence of surface states in the gap of the other III-V compounds is due to the relaxation of surface atoms. Low-energy electron diffraction (LEED) structural analysis has shown that the (110) surface is usually distorted with respect to the geometry of an ideal termination of the crystal, the metal atoms moving inward and the nonmetal atoms outward, in such a way that $1\times1$ surface periodicity is preserved.[5-7] The modifications in the electronic configuration occurring after this distortion are responsible for the removal of the dangling-bond surface state, found in the case of the ideal geometry, from the gap.[8-10]

Except for GaAs, where the structural analysis of the (110) surface is quite exhaustive, details of the lattice geometry near the surface for other III-V compounds are not so well defined. The main sources of experimental information on the surface atomic positions available for GaP(110) are electron paramagnetic resonance data for adsorbed $O_2^-$ species[11,12] and preliminary results[13] on elastic low-energy electron diffraction (ELEED) intensities. The surface relaxations suggested by these two methods are essentially the same, consisting in bond-length-conserving rotations within the surface layer. This model of relaxation is called rotation-relaxation (RR) model. A total energy minimization study,[12] based on a bond-orbital description of hybridization energy and on an elastic deformation model for the strain energy involved in the relaxation, has shown that the vertical displacements of the surface atoms occur without significant changes in bond length and that displacements of subsurface atoms are very small. These conclusions are in agreement with those achieved by the analysis of ELEED data, which suggest a value of 27.5° for the surface bond-rotation angle and do not show significant distortions in the positions of the atoms belonging to the second or third layer.[13] Figure 1 shows the relaxed geometry according to this model of relaxation.

From this structural information it seems possible to conclude that in GaP, unlike what happens in other III-V's, surface relaxation does not remove completely the surface states from the gap. Support to this conclusion has been given by theoretical calculations of the surface electronic structure performed by the authors[14] and by

 © 1981 The American Physical Society

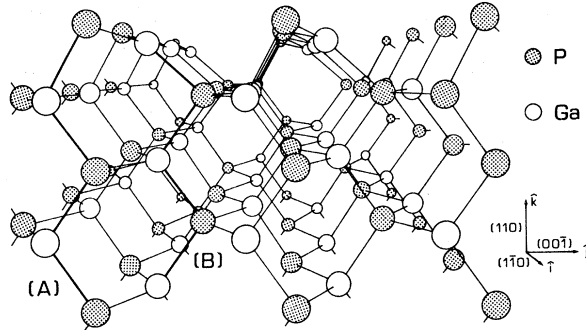


FIG. 1. Side view of a slab of five GaP(110) layers. The surface layer is relaxed according to the rotation-relaxation model with a surface bond-rotation angle $\theta$ =27.5°. Chains of atoms along a (1$\bar{1}$0) plane passing either through P (chain $A$) or through Ga (chain $B$) surface atoms are shown.

Nishida,[15] assuming several relaxed geometries. Both calculations rely upon a tight-binding description of the electron states, which has been used for a number of calculations of surface properties. While the method seems appropriate for the valence states, it does not provide an accurate description of the conduction band. This fact imposes a serious limitation on the conclusions drawn from tight-binding calculations about the empty surface states, which are mainly conduction-band derived. It is therefore interesting to perform a theoretical study of the electronic structure of this surface, using a method which does not suffer from these limitations. The pseudopotential method is particularly suitable to this purpose, since it is well known that it provides a realistic and accurate description of the bulk states.[16,17] This is specially true of empirically adjusted nonlocal pseudopotentials,[18] which yield bulk bands in very good agreement with the experimental data. However, these potentials are not suitable for a self-consistent calculation, since they cannot be partitioned in a bare potential and in a screening contribution, given as a functional of the valence charge density.[19] On the other hand, for the purpose of the present research, i.e., in order to establish whether the gap is free of intrinsic surface states, a local pseudopotential should prove satisfactory.

We have, therefore, undertaken a local pseudopotential study of the electron states at GaP(110) surface, performing a self-consistent calculation for the ideal and the relaxed configuration with a 27.5° rotation angle. Our results agree with those obtained in tight-binding calculations in that we find a nonvanishing density of surface states in the gap, but show significant differences in the nature and the location of the main surface states.

The plan of the paper is as follows: Sec. II presents the theoretical framework; Sec. III is devoted to the discussion of the pseudopotential used in the calculation and of the bulk band structure; the details of the surface calculations are given in Sec. IV, where a discussion of the self-consistent procedure is also presented. The results are displayed in Sec. V for both the atomic geometries. Section VI is devoted to the comparison with theoretical and experimental work. Possible improvements of the theory and future applications of the results are given in Sec. VII together with the conclusions.

## II. THEORETICAL FRAMEWORK

In this section we present the basic ideas underlying the method we used to calculate surface electron states. The method has been used in previous papers[20,21] and we refer to them for an extensive discussion. The key step of the procedure is to build up a periodical structure made of GaP slabs separated by regions of vacuum. Each slab is obtained by regularly stacking atomic planes and has a (110) surface on both sides. In our calculation we considered a repeated slab composed by nine GaP layers and six layers of vacuum. The introduction of the periodicity perpendicular to the surface plane allows us to employ bulk band structure techniques to derive the surface electronic properties.

The slab unit cell [orthorombic with $z$ axis perpendicular to (110) plane] has a volume 15 times larger than the bulk one. The mesh of reciprocal-lattice vectors is given by

$$\vec{G}=\frac{2\pi}{a}(\sqrt{2}n_1\hat{i}+n_2\hat{j}+\tfrac{2}{15}\sqrt{2}\,n_3\hat{k}), \quad (1)$$

$a$ being the bulk lattice constant and $\hat{i},\hat{j},\hat{k}$ the unit vectors of the axis of Fig. 1. The odd number of planes makes it possible to take advantage of the existence of reflection symmetry $z\rightarrow -z$ with respect to the central plane of the slab. An additional plane $yz$ of specular symmetry exists so that the point group of the repeated slab is $C_{2\nu}$. We fully exploited the symmetry of the system choosing for the slab calculation symmetry adapted combinations of plane waves as basis functions. This allowed us to reduce the size of the Hamiltonian matrix at high symmetry points $\bar{\Gamma},\bar{X},\bar{M},\bar{X}'$ of the two-dimensional Brillouin zone (2DBZ) and along $\bar{\Gamma}$-$\bar{X}'$ and $\bar{X}$-$\bar{M}$ directions, where the point group of wave vector $\vec{k}$ has four operations, by approximately four times and approximately two times elsewhere in the 2DBZ, where the $\vec{k}$-vector point group has two symmetry opera-

tions only. We considered up to 300 plane waves plus 1000 plane waves included via Löwdin second-order-perturbation technique.[22] These correspond to cutoff values of 2.7 and 7.0 Ry, respectively, and, as we will show in Sec. III, the number of plane waves is high enough to provide a good description of bulk bands.

The repeated slab scheme transforms a surface problem into a bulk one, therefore in the following we will describe the general features of our pseudopotential scheme valid for both the bulk and the surface calculations.

If the calculation has to be carried out self-consistently, three main ingredients are required. The first is the geometry of the system, specifying the periodicity and the location of the atoms in the unit cell. The second is a bare-ion pseudopotential, in our case the $Ga^{3+}$ and $P^{5+}$ ionic pseudopotentials, to be screened by the appropriate valence charge density in the iterative procedure, which leads to self-consistency. Lastly, we need some screened pseudopotential to use in the first step of the self-consistent procedure.

The geometry of the problem is described by the structure factor $S_i(\vec{G})$. Within the small core and local approximation, the bare pseudopotential is written as a superposition of ionic pseudopotentials,

$$V_b(\vec{r}) = \sum_{\vec{G}} \sum_i V_i(G) S_i(\vec{G}) e^{i\vec{G}\cdot\vec{r}} , \tag{2}$$

where $V_i(G)$ is the Fourier transform of the bare ionic pseudopotential

$$V_i(G) = \frac{1}{\Omega_a} \int d\vec{r}\, e^{-i\vec{G}\cdot\vec{r}} V_i(\vec{r}) \tag{3}$$

normalized to the atomic volume $\Omega_a$ (half of the bulk unit-cell volume).

We will discuss our choice of the bare pseudopotential in the next section together with the results for bulk GaP. As to the pseudopotential used to initiate the self-consistent process, its choice may depend upon the particular problem under consideration. Usually it is taken of the form

$$V_{(0)}(\vec{r}) = \sum_{\vec{G}} \sum_i W_i(G) S_i(\vec{G}) e^{i\vec{G}\cdot\vec{r}} , \tag{4}$$

where $W_i(G)$ is the screened single-atom form factor. This procedure, based on the concept of the superposition of linearly screened pseudoatoms, is a good start for a bulk calculation. In the surface case a large contribution arises from the existence of a potential barrier mainly due to exchange and correlation potential between the region of the crystal and the vacuum. As indicated in Sec. IV, an additional term must be included in the starting potential to describe the surface barrier correctly from the first iteration.

The eigenvalues and eigenfunctions are determined by diagonalizing the secular equation. The resulting wave functions are used to calculate the Fourier coefficients $\rho(\vec{G})$ of the total valence charge density, from which a Hartree potential is formed according to the Poisson equation

$$V_H(\vec{G}) = 4\pi e^2 \rho(\vec{G})/G^2 . \tag{5}$$

$\rho(\vec{G})$ has been evaluated by including high-symmetry-point contributions. For the bulk we considered $\Gamma, X, L, W$, and the midpoints of $\Sigma$ and $\Lambda$ directions. For the surface we took $\overline{\Gamma}, \overline{X}, \overline{X}'$, and $\overline{M}$ points of the two-dimensional Brillouin zone.

The knowledge of the valence charge density $\rho(\vec{r})$ allows us to derive the exchange and correlation potential in the form

$$V_{xc}(\vec{r}) = -\alpha \frac{3e^2}{2\pi} [3\pi^2 \rho(\vec{r})]^{1/3} . \tag{6}$$

To this end $\rho(\vec{r})$ has to be evaluated on a grid of about 80 000 points throughout the slab unit cell using fast-Fourier-transform algorithm. The cube root of $\rho(\vec{r})$ is evaluated at each grid point. The resulting function is transformed back into the reciprocal space, to give the Fourier coefficients $V_{xc}(\vec{G})$.

The sum of $V_H(\vec{G})$ and $V_{xc}(\vec{G})$ gives the Fourier coefficients of the screening potential. By adding it to the bare ionic pseudopotential, one forms the total crystal potential

$$V_T(\vec{G}) = V_H(\vec{G}) + V_{xc}(\vec{G}) + V_b(\vec{G}) . \tag{7}$$

To achieve self-consistency this potential is used to calculate new eigenvalues and eigenfunctions. With the wave functions a new screening potential is determined and another iteration starts. Care must be taken in performing this procedure, since instability problems can arise, particularly when dealing with surface calculations.[20,23,24] This point will be detailed later. The computing speed with which self-consistency is obtained depends upon the initial potential. It should be noted in this connection that the factorization of the Fourier transform of the total potential in structure factor and atomic form factors which is present in the initial potential $V_{(0)}$ does not exist in the successive iterations. From the physical point of view this is a consequence of the covalency of the chemical bond, i.e., of the contribution of multiple scat-

tering by different atoms in the unit cell to the one-electron wave function.[25,26]

## III. CHOICE OF IONIC PSEUDOPOTENTIAL AND BULK ELECTRONIC STRUCTURE

As indicated in the preceding section, the repeated slab method used to treat the surface problem requires the diagonalization of a large size matrix. The number of plane waves required is 15 times higher than in bulk calculation in order to have the same cutoff on $|\vec{k}+\vec{G}|^2$ in the evaluation of the matrix elements $\langle \vec{k}+\vec{G}'|W|\vec{k}+\vec{G}\rangle$ of the one-electron pseudopotential. The choice of the same cutoff and, more generally, the assumption of the same ingredients and of the same approximations in both bulk and surface calculations is necessary to have a meaningful comparison between the electronic structure of the surface and the bulk one. Furthermore, it is important to perform an accurate test of the potential and of the numerical method on the bulk problem before handling the surface problem.

The ionic potential, chosen among the different forms of pseudopotentials available at present, must be suitable for surface calculations with the same accuracy as in the bulk and it must provide a good description of the bulk band structure expecially in the gap region.

The maximum number of plane waves we can include in the calculation for the slab crystal is ~1300, this limit being essentially due to the size of the core memory and to the computing speed of the computer available (Cyber 76). This choice in the surface calculation corresponds to a cutoff value of 7.0 Ry in $|\vec{k}+\vec{G}|^2$ and, therefore, to a bulk calculation with a basis set of ~80 plane waves. Such a basis together with an appropriate choice of the bare ionic pseudopotential is sufficient to provide a good self-consistent description of the bulk bands.

Contemporary pseudopotentials which have been used in surface calculations can be roughly divided into two classes:

(i) model soft-core local pseudopotentials extensively used by the Berkeley group[20,21];

(ii) first-principles hard-core nonlocal pseudopotentials[27] used for GaAs by Zunger.[28]

The hard-core potentials of class (ii) have the advantage of being first-principles and fully nonlocal (i.e., the potential can be different for the different projections of the pseudowave on the states of different angular momentum). They have, however, the disadvantage of requiring a large number of plane waves (some hundreds) in bulk calculations because of their long tail in $\vec{G}$ space so that the comparison between bulk and surface calculations becomes problematic without a cutoff of the Fourier components of the ionic potentials. This shortcoming can be avoided by smoothing the potential in the core region. The softening of the core allows for a reasonable truncation in $\vec{G}$ space and simplifies the calculation. First-principles calculations performed up to now with these potentials do not give correct energy gaps for semiconductors. However, the failure has not to be attributed to the pseudopotentials but to the use of the density-functional approach in the description of the single-particle energies[29]: varying the exchange parameter $\alpha$ from the value $\alpha \simeq \frac{2}{3}$ to $\alpha \simeq 0.9$ generally improves the agreement with the experiments, leading to excellent gaps.

Simple analytical forms of the pseudopotential in reciprocal space have been used by the Berkeley group for calculations of Si,[20] GaAs and ZnSe surfaces,[21] and also interfaces.[30] The parameters appearing in those expressions were chosen to fit more complex-model potentials or to reproduce atomic eigenvalues. However, these authors did not show a detailed comparison between bulk and surface calculations obtained with the same ingredients.

In this work we have adopted a local form of the potential, which has an analytical expression in both real and reciprocal space. This form, due to Frensley and Kroemer,[31] is written as

$$V_i(r) = -\frac{e^2}{r}(Z_i - Q_i) + \frac{e^2}{r}\{Z_i \exp[-(Q_i/Z_i)^{1/2}\alpha_i r] + Q_i \exp(-\alpha_i r)\} + V_{0_i}\gamma_i^3(2\pi)^{-3/2}\exp(-\gamma_i^2 r^2/2)\,, \tag{8}$$

where $Q_i$ and $Z_i$ are the number of core electrons and the atomic number, respectively, $\alpha_i$ is fitted to the ionic charge distribution, and the two parameters $V_{0_i}$ and $\gamma_i$, appearing in the repulsive part, can be adjusted to obtain the electronic levels of the free ion or to reproduce directly the band structure of the solid.

The Fourier transform of the bare potential is given by

$$V_i(q) = -\frac{4\pi e^2}{\Omega_a}\left(\frac{Z_i - Q_i}{q^2} + \frac{Q_i}{q^2+\alpha_i^2} - \frac{Z_i}{(Q_i/Z_i)\alpha_i^2 + q^2}\right) + \frac{V_{0_i}}{\Omega_a}\exp\left(\frac{-q^2}{2\gamma_i^2}\right). \tag{9}$$

The values of the parameters for $Ga^{3+}$ and $P^{5+}$ are given in Table I. This potential corresponds to a core of intermediate softness and is rather similar to the first-principles $l=0$ and $l=1$ potentials in a large region of space.[28] The ionic potentials of Eq. (8) are shown in Fig. 2 together

TABLE I. Pseudopotential parameters of Ga and P ions used in Eq. (9). One-electron eigenvalues obtained for the potential of Eq. (9) (column A) and from the truncated approximation (column B). For a comparison with an *all-electron* calculation we report in column C the eigenvalues for the outer electron obtained by a Herman-Skillman calculation with $\alpha=1$ for $Ga^{2+}$ and $P^{4+}$.

| | | Potential parameters | | | |
|---|---|---|---|---|---|
| Ion | $Z$ | $Q$ | $\alpha_i$ $(a_0^{-1})$ | $V_{0i}$ $(\mathrm{Ry}\,a_0^3)$ | $\gamma_i$ $(a_0^{-1})$ |
| $Ga^{3+}$ | 31 | 28 | 3.64 | 30.5 | 2.0 |
| $P^{5+}$ | 15 | 10 | 4.99 | 41.0 | 2.5 |
| | | Energy eigenvalues (Ry) | | | |
| | | | A | B | C |
| Ga | 4$s$ | | −2.334 | −2.337 | −2.212 |
| | 4$p$ | | −1.653 | −1.656 | −1.646 |
| | 4$d$ | | −0.966 | −0.966 | −0.953 |
| | 5$s$ | | −1.031 | −1.029 | −1.009 |
| | 5$p$ | | −0.787 | −0.788 | −0.825 |
| P | 3$s$ | | −4.949 | −4.914 | −4.803 |
| | 3$p$ | | −3.891 | −3.915 | −4.026 |
| | 3$d$ | | −2.550 | −2.576 | −2.937 |
| | 4$s$ | | −2.373 | −2.323 | −2.349 |
| | 4$p$ | | −1.972 | −1.965 | −2.073 |

with those obtained by truncating the Fourier transform of Eq. (9) at $G_{\max}=4.34$ (a.u.)$^{-1}$ and coming back to real space. The comparison visualizes the effect of $\vec{G}$-space truncation which has been adopted in the computation. One can see that the two curves have nearly the same

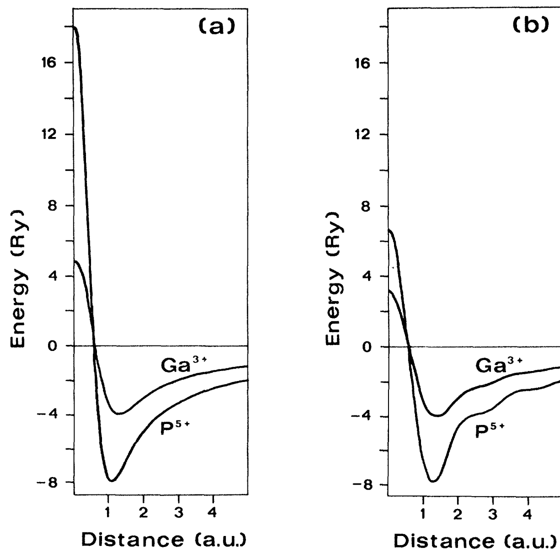


FIG. 2. Bare ionic pseudopotentials for $Ga^{3+}$ and $P^{5+}$ as obtained from Eq. (9) (a) and from the truncated approximation (b), plotted as functions of the distance from the nucleus.

"classical turning points" (i.e., crossing points of the $r$ axis) and the same depth of the minima. The main effect of the truncation is the slight shift of the minima toward higher distances from the nucleus and the introduction of a small oscillation, more evident in $P^{5+}$, around the Coulombic tail of the potentials. In Table I we also show how some energy eigenvalues of these potentials are varied by the truncation and how they compare with the energy eigenvalues obtained by an all-electron calculation of Herman-Skillman type.[32] We can remark that, as far as the energy eigenvalues are concerned, the effect of truncation is negligible (a maximum deviation of 0.2% or $2\times10^{-3}$ Ry for Ga and 0.8% or $3\times10^{-2}$ Ry for P). The agreement with the eigenvalues obtained by the atomic calculation is good, with special reference to the 4$p$ level of Ga. This turns out to be essential in order to get a good description of the bulk band gap. It is also possible to notice that the local approximation is rather appropriate for these pseudopotentials, since it gives reasonable results for eigenvalues of different angular momentum. The only obvious exception is the P 3$d$ level for which the pseudopotential coincides with the true ionic potential. The full test of the potentials used in the calculation is eventually the self-consistent bulk band structure they give. Figure 3 shows the GaP bulk band structure obtained with the potentials of Fig. 2 and with $\alpha=1$ in the expression of the exchange and correlation potential. This value corresponds to the original choice of Slater[33] and it is larger than those generally used at present. Many authors use the Kohn and Sham[34] value $\alpha=\frac{2}{3}$ or the value $\alpha=0.80$ suggested by $X\alpha$ method.[35] These choices do not give a good description of the gap between empty and filled states, because of the previously mentioned failure of the density-functional method. To overcome this difficulty it is convenient to choose an "effective" $\alpha$ in the range 0.9–1.0 to evaluate the exchange and correlation term according to Eq. (6).[36] Therefore, the old-fashioned $\alpha=1$ is more suitable to our purposes.

The obtained indirect band gap is 2.26 eV, the experimental value being 2.21 eV. The direct gaps $\Gamma_{15}\rightarrow\Gamma_1$, $L_3\rightarrow L_1$, $\Delta_5\rightarrow\Delta_1$, $\Gamma_{15}\rightarrow\Gamma_{15}$, and $L_3\rightarrow L_3$ are, respectively, 3.41, 3.51, 4.63, 4.82, and 6.48 eV against the experimental values 2.94, 3.79, 4.80, 5.19, and 6.70 eV. The larger deviation is the $\Gamma_{15}\rightarrow\Gamma_1$ gap, which is the feature mostly affected by the truncation of the potential. The other transitions are described with errors between 4% and 7%. The absolute gap is thus accurately reproduced and this is the main goal; the band structure as a whole compares favorably with the one of Ref. 18, which has been obtained

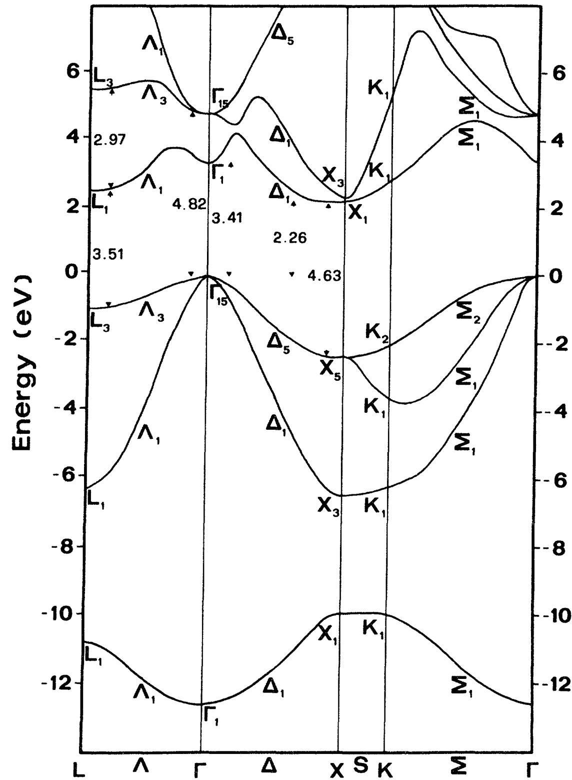

FIG. 3. Self-consistent bulk band structure of GaP.

by means of the empirical nonlocal pseudopotential method used to fit the experimental data.

Self-consistency in the bulk band-structure calculation, using Si empirical pseudopotential as starting potential, required eight iterations with differences of less than $10^{-5}$ Ry in the Fourier components of the total potential in the last two iterations.

In order to have a closer comparison between bulk and surface calculations we have solved the eigenvalue problem through a reduction of the Hamiltonian matrix size using the Löwdin second-order perturbation method to treat the plane waves with $2.7 \leq |\vec{k}+\vec{G}|^2 \leq 7.0$ Ry perturbatively. In this way the size of the matrix is ~24 in the bulk calculation. The eigenvalues are varied by a maximum of 0.02 eV with respect to the results of the full diagonalization all over the energy region indicated in Fig. 3. This result gives an estimate of the accuracy of the use of Löwdin procedure in the surface calculation.

In order to check the convergence in our calculations, we changed the number of plane waves in the expansion of the wave function, retaining the same cutoff in $\vec{G}$ space. We found excellent convergence in the calculated energy eigenvalues.

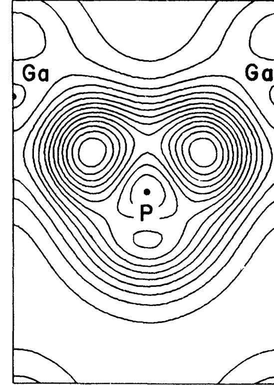

FIG. 4. Self-consistent pseudo-charge-density for bulk GaP along a $(1\bar{1}0)$ plane. The contours are spaced by 2.0 electrons per bulk unit cell.

The pseudo-charge-density obtained for the bulk in the (110) plane is displayed in Fig. 4. The pileup of charge along the bond directions is clearly visible. The agreement with the charge map obtained by the empirical pseudopotential method is quite good.[17] The maximum of the charge density along the bond is 32 $e$/cell. This picture of charge distribution is realistic outside the core region. Inclusion of the nonlocality or use of a hard-core potential can lead to modifications even in the bond region; however, these effects will not alter the conclusions about the comparison between bulk and surface charge distributions.

## IV. SELF-CONSISTENT PROCEDURE FOR THE REPEATED SLAB

As we mentioned in the previous sections, iteration in the self-consistent surface calculations may be a highly unstable procedure. This fact has been recognized by several authors[23,24] and various suggestions have been proposed in previous papers in order to dispose of this difficulty. The instability arises essentially from the low-$G$ behavior of the screening potential. $G$ vectors as short as 0.115 a.u. appear in the repeated slab calculation. The Fourier components of the potential at these small-$G$ vectors are not present in the bulk. They are extremely important in the surface case, since they determine the behavior of the surface potential barrier. Small changes in the screening potential at these $G$ vectors can give rise to significant modifications to the shape and height of the surface barrier and can introduce spurious fields with periodicity comparable with the slab size, caused by small deviations from local charge neutrality. These

effects arise both in the repeated slab and in semi-infinite crystal calculations.

If the starting potential is taken as a superposition of linearly screened atomic pseudopotentials or as empirical pseudopotential, as indicated in Eq. (4), the low-$G$ behavior of the input screening potential turns out to be extremely different from the one obtained after the first iteration, so that any simple iteration procedure, with standard damping techniques, does not converge. To avoid this difficulty, Schlüter and coworkers[20] have suggested a procedure which consists in systematically altering input and output screening potential until they are in essential agreement. This is done by inspecting $V_{out}$ versus $V_{in}$ separately for each small-$G$ component and with some sort of graphical interpolation between the calculated values. In successive applications of the method the small-$G$ components were also constrained to reproduce the experimental work function. The necessity of imposing this condition stems from the fact that work function and ionization potential are not obtained correctly by this way of treating the self-consistency. However, this procedure does not allow us to fix univocally the Fourier components of the pseudopotential, as the height of the surface barrier depends on all the low-$G$ coefficients. Therefore, it would be possible to get the same experimental work function with different sets of Fourier coefficients. Furthermore, it is our experience that this procedure does not permit the rapid achievement of self-consistency, which is desirable in these sorts of calculations. On the other hand, we feel that a good self-consistent calculation should give satisfactory values of the barrier height without imposing any constraints upon the screening potential, which automatically ensures agreement with the experimental data.

To find a more satisfactory and efficient procedure we notice that the factorization of the total potential in screened atomic pseudopotential and structure factor, while reasonably adequate to treat electrostatic contributions, is inappropriate when used in surface calculations, since it is highly inconsistent with the behavior of the exchange-correlation potential at the surface. Therefore, if starting potentials of the form given in Eq. (4) are used in the self-consistent procedure, the output potential of the first iteration turns out to be too different from the input potential to allow quick convergence.

This same instability has been found by Lang and Kohn[23] in their work on jellium. The contribution of the exchange and correlation potential to the jellium surface barrier at the electron density appropriate to GaP is indeed quite large, being 9.6 eV, nearly 60% of the total barrier-height. It is therefore important to treat this term correctly from the very beginning by including it in the starting potential of the self-consistent calculation.

According to these considerations we took our starting potential as

$$V_{(0)}(\vec{r})=\sum_{\vec{G}}\sum_{i} W_i(G)\, S_i(\vec{G})\, e^{i\vec{G}\cdot\vec{r}}+V_{xc}(z)\,, \tag{10}$$

where $V_{xc}(z)$ is the exchange and correlation potential of the jellium with the same density as GaP. The Fourier coefficients $W_i(G)$ have been chosen so that the factorized form $\sum_i W_i(G)\,S_i(\vec{G})$ would approximate as close as possible the Fourier components of the self-consistent bulk potential at the bulk $G$ vectors. For slab $G$ vectors lying between the bulk ones we have determined $W_i(G)$ by interpolation. For the small slab $G$ vectors, with $n_1=n_2=0$, whose modulus is less than the first bulk $G$, we interpolated between bulk values and the long-wavelength limit appropriate for linear metallic screening,[37] i.e., $\sum_i W_i(0)=-\frac{2}{3}E_F$. With this starting potential the self-consistent procedure can be carried out with the standard damped iteration technique, the input potential of stage $n$ being given in terms of input and output potentials of the previous stage $n-1$ by the expression

$$V_{in}(n)=\lambda_n V_{out}(n-1)+(1-\lambda_n)\,V_{in}(n-1)\,,\quad 0<\lambda_n\leq 1\,. \tag{11}$$

The parameter $\lambda_n$ is chosen according to the degree of agreement between $V_{out}(n-1)$ and $V_{in}(n-1)$. A typical value at the beginning of the iteration is $\lambda_1=0.1$, while at last stages $\lambda_n\sim 0.8$. Good convergence is achieved after seven to nine iterations. To illustrate this point we show in Fig. 5 the laterally averaged potentials

$$V(z)=\sum_{G_z} V(0,0,G_z)\, e^{iG_z z} \tag{12}$$

obtained from the input and output potentials at the last iteration and from our starting potential in the case of the relaxed surface. It is seen that the degree of agreement between input and output potentials at the last stage is quite relevant. No significant modifications in energies and wave functions occur in further stages of the procedure.

The surface barrier height obtained in this way is 1.18 Ry. This has to be compared with the value 1.09 Ry obtained by adding the experimental photoelectric threshold[1] to the difference between the top of the valence band and the bulk average potential. The agreement is good, considering

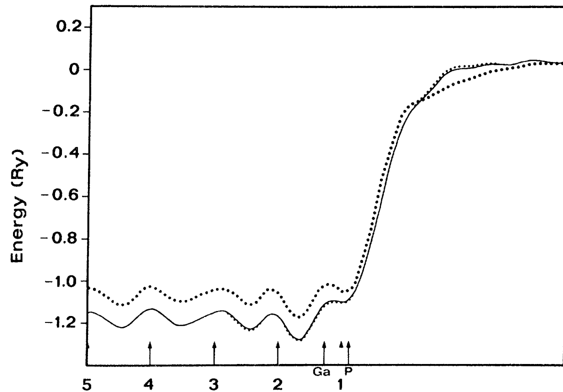


FIG. 5. Total laterally averaged potentials for relaxed GaP(110) surface. The input and output potentials of the last iteration (continuous and small-dotted line, respectively) are shown together with the starting potential of the self-consistent procedure (large-dotted line). The position of GaP layers and of the relaxed surface atoms are also indicated.

that our calculation is totally from first principles and we have not constrained the surface charge density to give the right work function.

Comparison with the starting laterally averaged potential shows that the self-consistent procedure leads to significant modifications of the potential in the internal layers too. This fact is not surprising in view of the inadequacy of the starting potential to represent covalency effects in the chemical bond. Such effects give rise to nonlinear screening contributions, not accounted for by the factorization. Indeed the iterative procedure gives a final potential, whose behavior in the internal planes is the same as the bulk self-consistent potential. Therefore we have a description of the repeated slab, which is completely consistent with that achieved in the bulk calculation.

## V. RESULTS

We calculated the surface band structure for both ideal and relaxed surfaces assuming the RR model with a bond rotation of 27.5°.[13] A detailed comparison between the results for the ideal and relaxed surface and the experimental data allows us to draw more definite conclusions on the surface geometry of the system. We start from a description of the results for the ideal geometry. Figure 6 shows the energy spectrum coming out of our self-consistent slab calculation for the ideal surface geometry at the high-symmetry points of the two-dimensional Brillouin zone. Surface states, identified through the localization of the wave function near the surface, are indicated by arrows and labeled by $A_i$ and $C_i$, depending on whether they are localized on the anions or cations, respectively. The subscripts used here are chosen in such a way as to simplify the comparison between the calculation for the ideal and relaxed surface geometry. Notice that surface

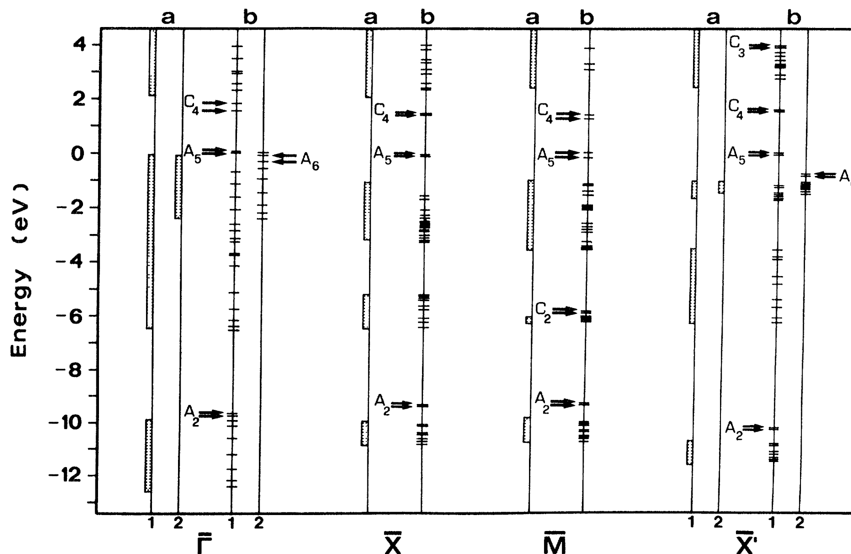


FIG. 6. Energy spectrum for GaP(110) ideal surface. Electron states are divided according to the representations of the point groups of the bulk directions corresponding to the high-symmetry points of the two-dimensional Brillouin zone. In column $a$ the projected bulk band structure is displayed. Column $b$ shows the eigenvalues resulting from the slab calculation. Surface states are indicated by arrows and labeled by $A_i$, $C_i$ according to the notation of Sec. V. Energies are referred to the top of the valence band.

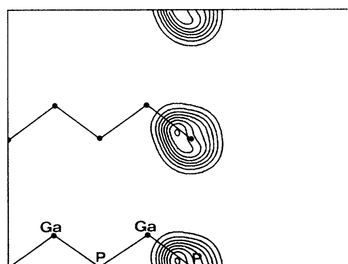


FIG. 7. Charge-density plot for surface state $A_2$ at $\overline{M}$ in the ideal geometry; the contours are spaced by 0.3 electrons per bulk unit cell.

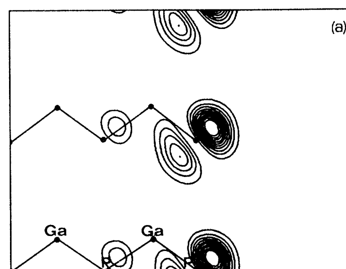


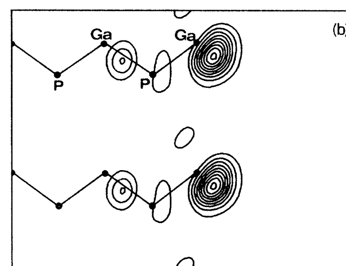


FIG. 9. Charge-density distribution for (a) filled surface state $A_5$ and (b) empty surface state $C_4$ at $\overline{M}$ point for the ideal geometry.

states always appear in couples due to the slab geometry exposing two surfaces to vacuum. Couples of surface states are almost degenerate, the degree of degeneracy being higher when the localization of surface states at the surface is stronger.

In the case of ideal geometry, surface states exist only in gaps and lenses of the projected bulk band structure (PBBS). The orbital character and the localization of surface states near the surface is illustrated by plotting the square modulus of the wave function along (110) planes perpendicular to the surface and passing through either Ga or P surface atoms. Figure 7 shows such a charge-density plot for the surface state labeled $A_2$, which is located near the lower edge of the ionic gap around $-9.8$ eV. This state is present at all symmetry points and appears to be a P-derived $s$ state strongly localized at the surface. A surface state of this kind has been found for the ideal (110) surface of all the other III-V zinc-blende semiconductors.[8,28,38]

Figure 8 shows the charge-density distribution for $C_2$, a surface state present at $\overline{M}$ point only, near the lower edge of the lens opening in the PBBS at the center of the Brillouin zone. It appears to be a Ga-derived $sp$ state. Figure 9 shows the charge-density distribution for $A_5$ and $C_4$, the dangling-bond states lying inside the fundamental gap, centered on P and Ga, respectively. The presence of such filled and empty surface states inside the gap is a very well-known characteristic of all the calculations of surface band structure for III-V's (Ref. 38) in the case of ideal geometry. A planar $p_x$ P-derived surface

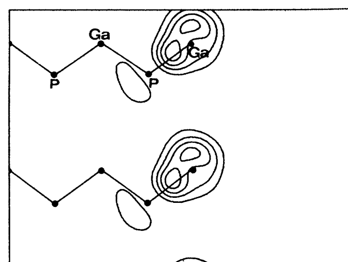


FIG. 8. Charge-density distribution of the surface state $C_2$ for ideal surface geometry at $\overline{M}$.

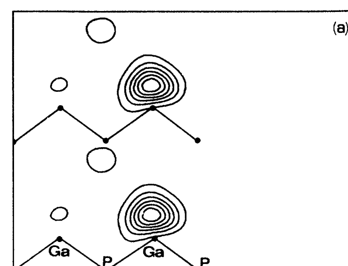


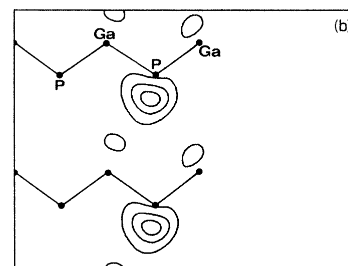


FIG. 10. Charge-density distribution for surface state $C_3$ at $\overline{X}'$ in the case of ideal surface geometry plotted along a $(1\overline{1}0)$ plane passing through P (a) and Ga (b) surface atoms.

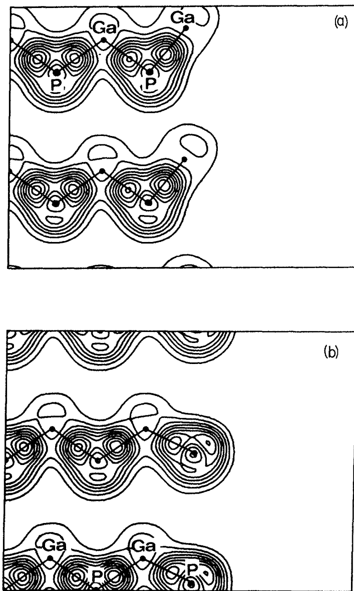


FIG. 11. Total valence charge density for relaxed GaP(110). The contours are spaced by 3.0 electrons per bulk unit cell.

state $A_6$ exists at $\bar{\Gamma}$ and $\bar{X}'$ just below the valence-band maximum. Finally $C_3$ (Fig. 10) located at 3.98 eV at $\bar{X}'$ is localized on the Ga atoms of the second layer with a non-negligible contribution from P-derived states.

Let us turn now our attention to the results for the relaxed surface. In Fig. 11 we display the total self-consistent valence charge density plots for GaP(110) relaxed surface. The perturbation induced by the surface extends up to two layers and manifests itself only in a change of shape: The pileup of charge along the bonds between Ga and P is essentially the same in the surface region as in the bulk. It should be mentioned that this is not the case for the ideal surface where the value of the bonding charge at the surface differs more from the bulk value than in this case. This fact, as it has been noted for GaAs,[9] is a positive test of the greater stability of the relaxed surface compared with the ideal one.

Figure 12 shows the energy spectrum calculated for the relaxed surface geometry. Again $A_i$ and $C_i$ label the anion- and cation-derived surface states. The surface band structure is considerable different from the ideal case: All the surface states found for the ideal geometry are still present in the relaxed surface but at different energies; moreover, due to the difference between the geometrical array of the atoms at the surface and in the first sublayer, many new surface states and resonances with maxima of electronic charge in the first two layers appear either in gaps of the PBBS or degenerate with the bulk continuum. This is the case of the strong surface state $A_1$ near the bottom of the valence band around − 11.0 eV. It is present at all the high symmetry points except $\bar{\Gamma}$ where it becomes a very weak resonance. Its charge-density distribution in Fig. 13 allows to identify it as a second-layer P-derived $s$ state.[39]

State $A_2$ charge-density plot is displayed in Fig. 14 and appears to be the same P-derived $s$ state as in the ideal surface. The same can be said for $C_2$ (Fig. 15), an $sp$ Ga-derived state

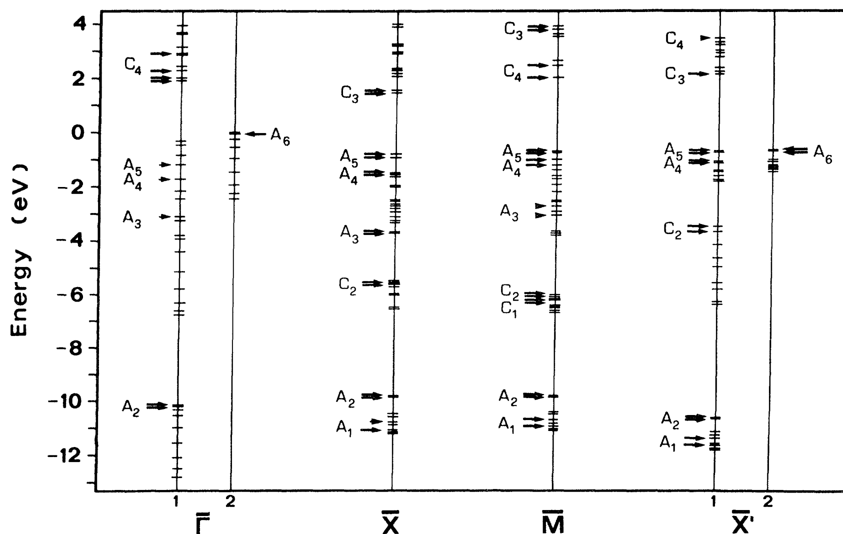


FIG. 12. Energy spectrum for relaxed GaP(110) surface at high-symmetry points. Surface states and resonances are indicated by arrows and dotted arrows, respectively.

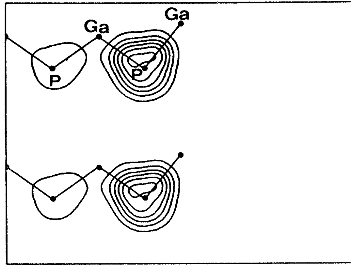


FIG. 13. Charge-density plot for $A_1$ at $\bar{X}$ point for the relaxed geometry.

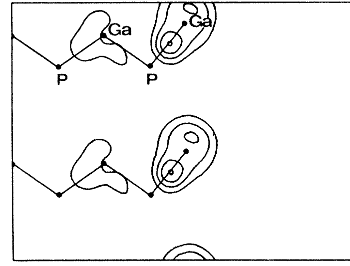


FIG. 15. Charge-density plot for state $C_2$ at $\bar{M}$ point in the relaxed surface case.

also present in the ideal case, which now extends to $\bar{X}$ and $\bar{X}'$ following the lower edge of the internal gap. $C_1$, on the contrary, is a new surface state induced by relaxation, localized on the Ga atoms of the first sublayer with predominant $s$ character (Fig. 16). It is present only at $\bar{M}$ point. Near the upper edge of the internal gap at $\bar{X}$ point a strong surface state $A_3$ arises upon relaxation (Fig. 17). It is a well-defined $p_y$ state localized on the first sublayer anions and becomes a weak resonance on moving toward $\bar{\Gamma}$ and $\bar{M}$.

We are now approaching the valence-band maximum, where we find a couple of surface states $A_4$ and $A_5$ shown in Fig. 18. $A_5$ is the P-derived dangling-bond state already found in the ideal case. Its energy position is now considerably lower than in the ideal surface so that it lies completely out of the gap. $A_4$ is a P-derived $p_y p_z$ back-bond state located between $-1.7$ and $-1.1$ eV. Both $A_4$ and $A_5$ are present at all the high-symmetry points. State $A_6$ appears only at $\bar{\Gamma}$ and $\bar{X}'$ and is a planar $p_x$ state.

As already predicted by tight-binding studies,[14] relaxation is not able to remove empty surface states from the gap: $C_3$ and $C_4$, whose charge-density plots are shown in Fig. 19, occupy the upper part of the gap interchanging their relative positions at different points of the Brillouin zone.

$C_4$ is the dangling-bond Ga-derived state already found for the ideal surface which now has been pushed up at $\bar{\Gamma}, \bar{X}, \bar{X}'$ and down in energy at $\bar{M}$ by relaxation. $C_3$ is a back-bond state which overlaps the gap region, except at $\bar{M}$ where it lies higher than $C_4$. The presence of this state in the gap is the consequence of rehybridization, which occurs at the surface, and can pull back-bond states out of the conduction-band bottom.[40]

Table II summarizes the energy positions of surface states at the high-symmetry points, together with parity under mirror-plane reflection $x \rightarrow -x$. Mirror-plane-symmetry properties of surface states can be experimentally defined by angle-resolved polarization dependent photoemission experiments. Such data, now available for GaAs (Ref. 41) only, can be useful in a comparison between theoretical results and experimental data.

## VI. COMPARISON WITH PREVIOUS WORK

In this section we compare our results with previous theoretical work and with the experimental data available for GaP(110) surface. The overall picture of surface electronic structure we have been describing here is similar to the one coming out from previous tight-binding calculations.[14] Surface states for the *ideal* geometry are in both cases located inside the gap of the

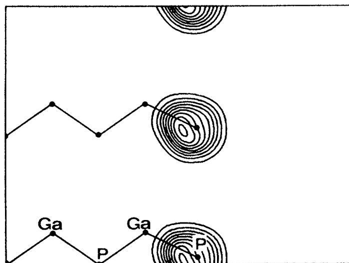


FIG. 14. Charge-density plot for state $A_2$ at $\bar{M}$ point in the case of relaxed geometry.

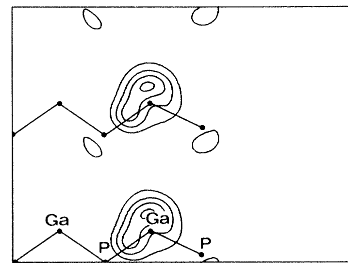


FIG. 16. Charge-density distribution of surface state $C_1$ in the relaxed surface case.

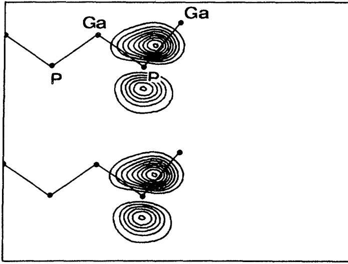


FIG. 17. Surface state $A_3$ charge-density plot at $\bar{X}$ point.

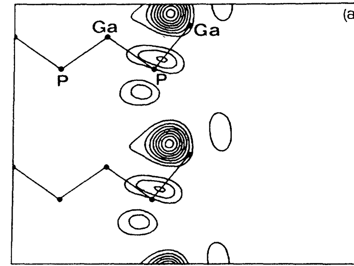


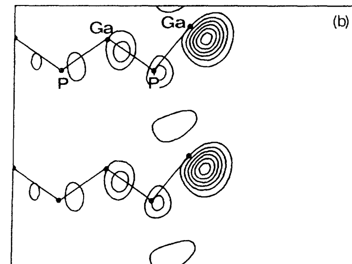


FIG. 19. Charge-density distribution for (a) $C_3$ and (b) $C_4$ surface states at $\bar{M}$ point.

PBBS and their orbital character and energy position are quite similar, in spite of the difference of the description of the bulk bands given by the two methods. Tight-binding results for the *relaxed* surface are only available for the RR model with $\theta=34.8°$ and $\theta=20°$. All the same the main surface features obtained by tight binding are comparable with the ones obtained in the present calculation even if the details of the electronic structure, in terms of energy position, surface band dispersion, and symmetry ordering of surface states, being sensible to the surface geometry, are somewhat different.

Four surface states are in both cases located in the gap region, the two filled ones out of the gap and the empty ones still inside the gap. It should be mentioned that filled surface state bands obtained by tight binding have the same orbital character and ordering as in pseudopotential calculation. For tight-binding results the orbital composition of the empty states is somewhat different, although they seem to rise from dangling- and back-bond states.

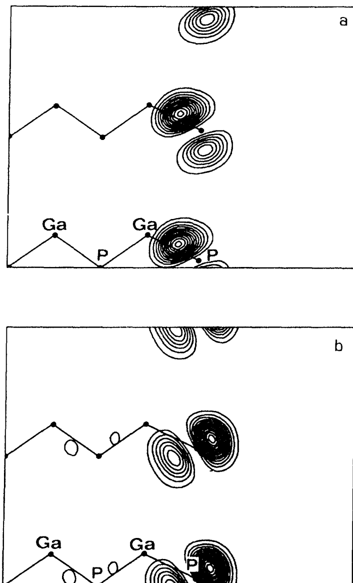


FIG. 18. Charge-density plots for (b) the dangling-bond surface state $A_5$ and (a) back-bond surface state $A_4$ at $\bar{X}$ point.

The main difference between the two calculations arise in the lower part of the energy spectrum. Tight-binding calculations involving no bond-length changes do not predict any surface state at the bottom of the valence band as the pseudopotential does. Moreover, the surface Ga-derived state given by tight binding at $\bar{M}$ point partially overlapping the ionic gap is totally absent in pseudopotential calculation.

Cluster calculations performed using the extended Hückel method[15] yield an empty dangling-bond surface state in the gap of dominant Ga character in the relaxed surface. Unlike the present calculation and the outcome of the tight-binding studies, there is no overlap between the back-bond surface state and the gap. At present it is not clear whether this discrepancy arises from the use of a cluster of atoms to simulate the bulk or from some inadequacy of the extended Hückel method in approaching the main features of the conduction band.

As we mentioned previously, the pseudopotential approach has been used to perform calculations similar to those presented in this paper, mainly for GaAs. Calculations with a local pseudopotential[9,21] give results quite close to ours, the main surface features having the same composi-

TABLE II. Energy positions referred to the valence-band maximum and parity with respect to mirror-plane symmetry of surface states found in the case of relaxed surface geometry at the high-symmetry points of the two-dimensional Brillouin zone.

| | $\bar{\Gamma}$ | | $\bar{X}$ | | $\bar{M}$ | | $\bar{X}'$ | |
|---|---|---|---|---|---|---|---|---|
| | eV | Parity | eV | Parity | eV | Parity | eV | Parity |
| $A_1$ | | | −10.95 | odd | −10.87 | odd | −11.75 | even |
| $A_2$ | −10.17 | even | −9.87 | even | −9.85 | even | −10.74 | even |
| $A_3$ | −3.13 | even | −3.22 | odd | −2.93 | odd | | |
| $A_4$ | −1.72 | even | −1.62 | even | −1.12 | even | −1.24 | even |
| $A_5$ | −1.20 | even | −0.88 | even | −0.74 | even | −0.80 | even |
| $A_6$ | −0.06 | odd | | | | | −0.77 | odd |
| $C_1$ | | | | | −6.20 | even | | |
| $C_2$ | | | −5.59 | odd | −6.09 | odd | −3.76 | even |
| $C_3$ | 1.96 | even | 1.53 | odd | 3.87 | odd | 2.10 | even |
| $C_4$ | 2.63 | even | | | 2.21 | odd | 3.35 | even |

tion and symmetry. A nonlocal calculation has been carried out by Zunger,[28] assuming the same geometry of Ref. 21, for GaAs. The results show some differences with respect to those of the local theory, the most important being the presence of an additional As-derived state at ~3 eV below the valence-band maximum, a strong $d$ contribution in the empty surface bands near the conduction-band minimum, and a higher binding energy for the lowest As ($s$-derived) states near the valence-band bottom. The overall picture seems to be in better agreement with the experiments than the one provided by the local theory. A similar calculation for GaP(110) would probably yield similar differences with respect to the results of the present paper, particularly in the description of the lowest valence states, which are better described by the nonlocal theory, due to a more accurate description of the valence band.

We turn now to the comparison of our results with the experimental information. Most of the experimental work on GaP(110) surface has been focused on the detection of intrinsic states in the gap. To this end contact potential difference and photoelectron spectral distribution measurements have been performed[1,2] to show Fermi-level stabilization. For $n$-type samples pinning occurs at 1.65–1.7 eV above the valence-band maximum, which can be caused by the lower edge of intragap band of surface states. Our results agree with this conclusion: The lower edge of the empty surface band lies at about 1.53 eV above the valence-band maximum near $\bar{X}$ point. It has a clear back-bond character and is the bottom of the back-bond surface band. Partial-yield spectroscopy with ultraviolet photoemission[3,4] shows a transition from the spin-orbit split Ga 3$d$ levels to empty surface states. The transitions occur at 19.7 and 20.2 eV and the final-state energy is 1.3 eV above the valence-band maximum. Taking account of the excitonic effects, an excitonic binding energy as large as ~1 eV would be required to locate the final state out of the gap. Values of ~0.5 eV give a better estimate of this energy in other III-V compounds.[1-3] It seems, therefore, rather likely that the transition observed would involve a final state in the gap. Since our empty surface bands are mainly located around 1.9–2.1 eV, the estimated exciton binding energy from our results is around 0.6–0.8 eV, so that our picture is consistent with the experimental information.

Energy-loss spectra have been used to derive an approximate energy-levels diagram consistent with the other experimental data for all the III-V's.[4] In the case of GaP(110) the proposed surface-state positions referred to the valence-band maximum are −10.5, −6.5, −1.2, 2.2, and 8.5 eV. Such assignments are consistent with the results obtained by the method of the fractional change of external reflectivity,[42] which shows a surface optical transition at ~3.4 eV in GaP. Our description of the filled surface states gives a band in the range −1.1–1.7 eV and two bands between −9.8 and −10.8 eV, in agreement with previous assignments. Surface states located between −5.6 and −6.2 eV are found at $\bar{X}$ and $\bar{M}$ points near the lower edge of the lens in the PBBS. As to the surface structure observed in optical spectra at 3.4 eV,[42] it can be ascribed to a transition from P-derived filled states between −1.2 and −1.5 eV to the empty Ga-derived states in the band gap. Such an assignment was proposed in the experimental work and our calculation gives substantial support to it. A more detailed test of the theory, especially of our description of the filled states, could be provided by angle-resolved photoemission experiments like the ones performed on GaAs.[41]

ACKNOWLEDGMENTS

We thank Dr. A. Kahn for his preliminary data about the LEED structural analysis of GaP. All the calculations were performed at the Centro di Calcolo, Università di Modena, whose technical assistance and financial support is gratefully acknowledged. In particular we thank Dr. R. Zanasi for supplying the plotting routines.

---

[1]A. Huijser, J. van Laar, and T. L. van Rooy, Surf. Sci. 62, 472 (1977); A. Huijser, Ph.D. thesis, Techische Hogeschool, Eindhoven, 1979 (unpublished).
[2]G. M. Guichar, C. A. Sebenne, and C. D. Thuault, J. Vac. Sci. Technol. 16, 1212 (1979).
[3]D. E. Eastman and J. L. Freeouf, Phys. Rev. Lett. 34, 1624 (1975); D. Norman, I. T. McGovern, and C. Norris, Phys. Lett. 63A, 384 (1977).
[4]H. Lüth and G. J. Russel, Surf. Sci. 45, 329 (1974); J. van Laar, A. Huijser, and T. L. van Rooy, J. Vac. Sci. Technol. 14, 894 (1977); R. Ludeke and A. Koma, *ibid.* 13, 241 (1976).
[5]A. R. Lubinsky, C. B. Duke, B. W. Lee, and P. Mark, Phys. Rev. Lett. 36, 1058 (1976).
[6]S. Y. Tong, A. R. Lubinsky, B. J. Mrstik, and M. A. van Hove, Phys. Rev. B 17, 3303 (1978).
[7]C. B. Duke, R. J. Meyer, A. Paton, P. Mark, A. Kahn, E. So, and J. L. Yeh, J. Vac. Sci. Technol. 16, 1252 (1979).
[8]C. Calandra, F. Manghi, and C. M. Bertoni, J. Phys. C 10, 1911 (1977).
[9]J. R. Chelikowsky and M. L. Cohen, Phys. Rev. B 20, 4150 (1979).
[10]D. J. Chadi, J. Vac. Sci. Technol. 15, 1244 (1978); Phys. Rev. B 18, 1800 (1978).
[11]D. J. Miller and D. Haneman, J. Vac. Sci. Technol. 15, 1267 (1978).
[12]D. J. Miller and D. Haneman, Surf. Sci. 82, 102 (1979).
[13]A. Kahn, private communication.
[14]C. M. Bertoni, O. Bisi, F. Manghi, and C. Calandra, J. Vac. Sci. Technol. 15, 1256 (1978).
[15]M. Nishida, Solid State Commun. 28, 551 (1978).
[16]M. L. Cohen and T. K. Bergstresser, Phys. Rev. 141, 789 (1966).
[17]J. P. Walter and M. L. Cohen, Phys. Rev. B 4, 1877 (1971).
[18]J. R. Chelikowsky and M. L. Cohen, Phys. Rev. B 14, 556 (1976).
[19]A. Zunger and M. L. Cohen, Phys. Rev. B 20, 4082 (1979); A. Zunger, *ibid.* 21, 4785 (1980).
[20]M. Schluter, J. R. Chelikowsky, S. G. Louie, and M. L. Cohen, Phys. Rev. B 12, 4200 (1975).
[21]J. R. Chelikowsky and M. L. Cohen, Phys. Rev. B 13, 826 (1976).
[22]P. O. Löwdin, J. Chem. Phys. 19, 1936 (1951).
[23]N. D. Lang and W. Kohn, Phys. Rev. B 1, 4555 (1970).
[24]G. Alldredge and L. Kleinman, Phys. Rev. B 10, 559 (1974).
[25]K. H. Benemann, Phys. Rev. 133A, 1045 (1964).
[26]C. M. Bertoni, V. Bortolani, C. Calandra, and F. Nizzoli, J. Phys. C 6, 3612 (1973).
[27]A. Zunger and M. L. Cohen, Phys. Rev. B 18, 5449 (1978).
[28]A. Zunger, Phys. Rev. B 22, 959 (1980).
[29]D. R. Hamann, Phys. Rev. Lett. 42, 662 (1979); A. Zunger, Phis. Rev. B 21, 4785 (1980).
[30]J. Ihm and M. L. Cohen, Phys. Rev. B 20, 729 (1979).
[31]W. R. Frensley and H. Kroemer, J. Vac. Sci. Technol. 13, 810 (1976); Phys. Rev. B 16, 2642 (1977); Appl. Phys. Lett. 31, 46 (1977).
[32]F. Herman and S. Skillman, *Atomic Structure Calculations* (Prentice-Hall, Englewood Cliffs, 1963).
[33]J. C. Slater, Phys. Rev. 81, 385 (1951); 82, 538 (1951).
[34]W. Kohn and L. Sham, Phys. Rev. 170, 1133 (1965).
[35]J. C. Slater, J. Chem. Phys. 43, S228 (1965).
[36]D. J. Stuckel and R. N. Euwema, Phys. Rev. B 1, 1635 (1970); T. C. Collins, D. J. Stuckel, and R. N. Euwema, *ibid.* 1, 724 (1970); K. Mednick and C. C. Lin, *ibid.* 17, 4807 (1978).
[37]W. A. Harrison, *Pseudopotentials in the Theory of Metals* (Benjamin, New York, 1966).
[38]C. M. Bertoni, O. Bisi, C. Calandra, and F. Manghi, *Physics of Semiconductors, 1978,* edited by B. L. H. Wilson (Institute of Physics, London 1979), pp. 191–194.
[39]This state arises here from a surface atomic distortion which preserves the ideal (bulk) bond length. A similar state has been found in a pseudopotential calculation for relaxed GaAs(110) (Ref. 9) using a geometry which involves bond length changes. The presence of this state and its subsequent experimental detection has been considered a direct evidence for a bond length change occurring between the first layer and the substrate. If our results for GaP can be extrapolated, as it seems reasonable, to GaAs, this argument loses its validity.
[40]W. H. Harrison, *Electronic Structure and the Properties of Solids* (Freeman, San Francisco, 1979).
[41]G. P. Williams, R. J. Smith, and G. J. Lapeyre, J. Vac. Sci. Technol. 15, 1249 (1978).
[42]P. Chiaradia, G. Chiarotti, F. Ciccacci, R. Memeo, S. Nannarone, P. Sassaroli, and S. Selci, Surf. Sci. 99, 70 (1980).